

Assessing the causal effects of a stochastic intervention in time series data: Are heat alerts effective in preventing deaths and hospitalizations?

Xiao Wu

Department of Biostatistics, Harvard T.H. Chan School of Public Health
and

Kate R. Weinberger

School of Population and Public Health, University of British Columbia
and

Gregory A. Wellenius

Department of Environmental Health,
Boston University School of Public Health
and

Francesca Dominici, Danielle Braun

Department of Biostatistics, Harvard T.H. Chan School of Public Health

February 23, 2021

Abstract

We introduce a new causal inference framework for time series data aimed at assessing the effectiveness of heat alerts in reducing mortality and hospitalization risks. We are interested in addressing the following question: how many deaths and hospitalizations could be averted if we were to increase the frequency of issuing heat alerts in a given location? In the context of time series data, the overlap assumption – each unit must have a positive probability of receiving the treatment – is often violated. This is because, in a given location, issuing a heat alert is a rare event on an average temperature day as heat alerts are almost always issued on extremely hot days. To overcome this challenge, first we introduce a new class of causal estimands

under a stochastic intervention (i.e., increasing the odds of issuing a heat alert) for a single time series corresponding to a given location. We develop the theory to show that these causal estimands can be identified and estimated under a weaker version of the overlap assumption. Second, we propose nonparametric estimators based on time-varying propensity scores, and derive point-wise confidence bands for these estimators. Third, we extend this framework to multiple time series corresponding to multiple locations. Via simulations, we show that the proposed estimator has good performance with respect to bias and root mean squared error. We apply our proposed method to estimate the causal effects of increasing the odds of issuing heat alerts in reducing deaths and hospitalizations among Medicare enrollees in 2817 U.S. counties. We found weak evidence of a causal link between increasing the odds of issuing heat alerts during the warm seasons of 2006-2016 and a reduction in deaths and cause-specific hospitalizations across the 2817 counties.

Keywords: Multiple time series; Propensity score; Time-varying confounding

1 Introduction

Extreme heat events are widely recognized as a significant threat to public health (US EPA 2006). In the U.S., heat waves have been associated with very high morbidity and mortality (Bobb et al. 2014, Weinberger et al. 2020). In an effort to reduce heat-related mortality and morbidity, the U.S. National Weather Service (NWS) issues heat alerts in advance of forecast extreme heat events in order to communicate these risks to the public and local government officials (Hawkins et al. 2017). However, it is largely unknown how effective these heat alerts are in reducing adverse health outcomes such as deaths and hospitalizations. To fill these knowledge gaps, we acquired daily time series data on: 1) daily maximum heat index (an index that combines air temperature and relative humidity to posit a human-perceived equivalent temperature); 2) issuance of heat alerts; and 3) number of deaths and hospitalizations among Medicare enrollees for 2817 U.S. counties within the warm season (April-October) from 2006 to 2016 (a total of 2354 days).

Although randomized controlled experiments are considered the gold standard for evaluating the effectiveness of public policy (Athey & Imbens 2017), it would be unethical to conduct them in this context since randomly suspending the heat alert system may result in excess deaths attributable to heat (Weinberger et al. 2018, Benmarhnia et al. 2016). Therefore, evaluating the effectiveness of NWS-issued heat alerts can only be conducted by analyzing observational data. In our time series data, the treatment (e.g., the issuance of a heat alert on a given day in a county) is determined by an unknown assignment mechanism rather than by controlled randomization. Consequentially, to eliminate confounding bias, we must control for time varying covariates that are associated with both the treatment (e.g., issuance of heat alerts) and outcomes of interest (e.g., deaths or hospitalizations). In addition, to reliably estimate causal effects such as the average treatment effect (ATE), i.e., the contrast of the potential outcome under a treatment $W = 1$ vs. $W = 0$ ($ATE(1, 0) = E[Y(1) - Y(0)]$), the overlap assumption must be met, that is, any unit (e.g., an observation for a given location on a given day) must have a positive probability of receiving either treatment or control (Rosenbaum & Rubin 1983). In our

context, this assumption is likely violated because the assignment to the treatment is rare and unbalanced. Indeed, the issuance of a heat alert takes place on average in 2.52 % (standard deviation: 2.19 %) of the warm season days across U.S. counties. Moreover, a heat alert is highly unlikely on a relatively cool day, whereas it almost always happens on very hot days. Even if the overlap assumption holds with limited overlap (i.e., chances of assigning to the treatment are merely small), a large sample size is needed to learn about all possible treatment assignments and avoid large estimated variance (Kang et al. 2007).

Causal inference in the context of time varying treatments has been extensively studied in longitudinal settings by Robins & Hernán (2009) where the unit of the analysis is the person or the location (e.g., a county) and often the number of units (N) is much larger than the number of repeated observations (T) for a single person or location. In contrast, our data set presents the unique feature of time series, where the unit of the analysis is the observation for a given day in a given county and the number of days for a single time series might be much larger than the number of counties, that is $T > N$. Furthermore, it is plausible that the true causal effects might be highly heterogeneous across counties. This presents a huge challenge: the causal estimand defined on a super-population, e.g., an ATE with respect to large N (e.g., counties), might not capture the heterogeneous nature of each county and cannot be estimated without stringent assumptions regarding model extrapolation. Therefore, careful thought and consideration should be given to account for heterogeneous causal effects across multiple counties.

Previous research has focused on some aspects of the methodology gaps mentioned above. Research on confounding adjustment in observational studies has relied extensively on the propensity score, that is, the probability of a unit being assigned to a particular treatment given other pre-treatment covariates (Rosenbaum & Rubin 1983). Often, confounding adjustment via propensity scores is used when the goal of the inference is to estimate a causal effect of a deterministic intervention. That is, under a situation where each unit's treatment can have a fixed value (e.g., treatment $W = 1$ or control $W = 0$) such as in the context of the ATE. Such estimands compare potential outcomes if units were

deterministically assigned treatment $W = 1$ vs. control $W = 0$. The overlap assumption, which is unlikely to hold in our setting, plays a central role when identifying the causal estimands under deterministic interventions. Stochastic interventions (e.g., changing the probability of being assigned to a given treatment in some pre-specified way) have been previously defined to help overcome violations of the overlap assumption (Haneuse & Rotnitzky 2013, Kennedy 2019, Naimi et al. 2021). Kim et al. (2019) have shown that a stochastic intervention framework and its corresponding causal estimand is appealing when the study contains long time periods (large T), as in our context. However, properties of this framework have only been demonstrated in the context of asymptotic arguments with respect to large sample size N in longitudinal settings. In other words, previous approaches (Kim et al. 2019) were designed to analyze longitudinal studies when N goes to infinity rather than time series studies when T goes to infinity. The causal inference literature on time series studies is sparse with a few exceptions (Bojinov & Shephard 2019, Papadogeorgou et al. 2020). Bojinov & Shephard (2019) only focused on the randomized experiment setting and proposed an ATE-type causal estimand under deterministic interventions, which does not directly apply to our observational data. Papadogeorgou et al. (2020) is the first to bridge stochastic intervention framework with observational spatial-temporal data, but they focused on spatio-temporal point processes which are suitable for modelling a single time series with a common treatment (e.g., airstrikes) rather than multiple time series with different treatment paths from heterogeneous sources (e.g., heat alerts issued by local NWS offices).

To the best of our knowledge, no existing causal inference approach answers causal questions defined by stochastic interventions under observational data that consists of multiple time series. In this paper we introduce a novel statistical framework in the context of a stochastic intervention for time series data. The key idea is to replace a deterministic intervention (i.e., issuing vs. not issuing a heat alert on day t , deterministically) by a stochastic intervention (i.e., increasing the odds of issuing a heat alert on day t by a ratio δ_t). Specifically, *our proposed incremental intervention characterizes an increased odds to*

treat (e.g., issuing a heart alert) by δ_t -fold at time t conditional on past information up to time t . This novel causal inference framework allows us to define causal estimands on time series data and ease the identification and estimation difficulties due to the violation of overlap assumption. Based on this framework, we further define a broad class of stochastic causal estimands and propose nonparametric estimators based on time-varying propensity scores to estimate such causal effects from observational data.

In Section 2, we discuss the national heat alert, heat index and Medicare data that motivate our methodological developments. In Section 3, starting in the context of a single time series, we define the stochastic causal estimands based on incremental propensity score interventions, and their corresponding assumptions for their identification. In Section 4, we propose nonparametric estimators based on time-varying propensity scores. In Section 5, we extend our approach in the context of multiple time series, we introduce additional identification assumptions, and propose a random-effect meta-analysis to pool causal estimands across time series from multiple locations. In Section 6, we illustrate the finite-sample performance of the proposed estimators via simulation studies. In Section 7, we apply our method to the national heat alert data set to estimate the effectiveness of heat alerts in reducing morbidity and mortality among Medicare beneficiaries. In Section 8, we conclude with a summary and discussion.

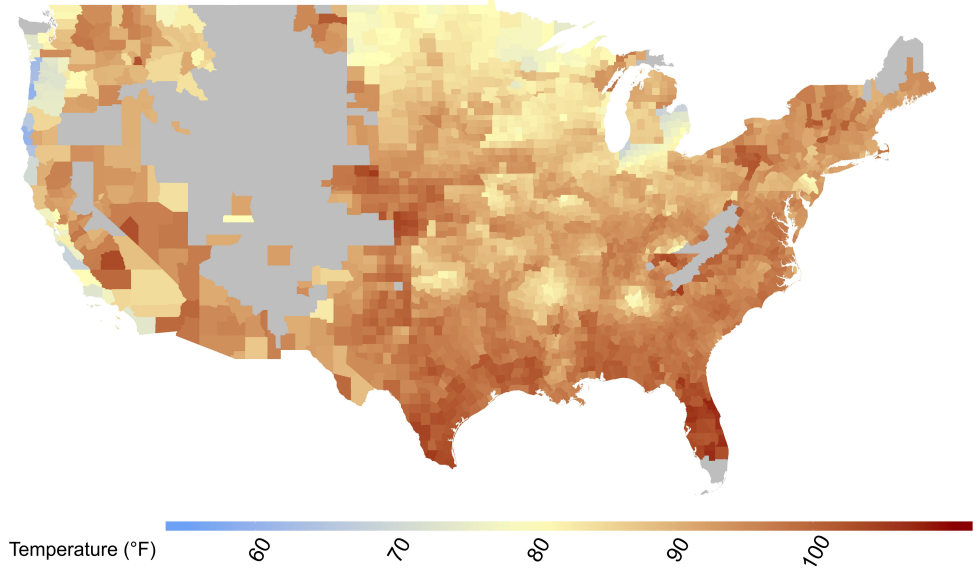
2 Motivating Data

For this study, we gathered text files containing records of all non-precipitation alerts issued by NWS between 2006 and 2016 from the National Oceanic and Atmospheric Administration (NOAA). We used the information in the file header, which contains information on the type, location, and timing of each alert in a standard format, to identify the date and location of each heat alert issued between April 1st and October 31st for the years 2006 to 2016 in the contiguous U.S.. We then created a daily time series containing a binary variable for the issuance of heat alerts for each of the 2817 U.S. counties. We defined “heat alerts” to include both heat advisories (a type of heat alert issued when less severe heat is

forecast) and excessive heat warnings (a type of heat alert issued when more severe heat is forecast). While the exact criteria used to issue heat alerts varies across the jurisdictions of local NWS offices, a key commonality across jurisdictions is that heat alerts are issued based on forecasts of future weather conditions (mainly, heat index). Furthermore, in addition to using information from forecast models, NWS forecasters are encouraged to use their experience and judgment in deciding whether or not to issue a heat alert (Hawkins et al. 2017). In summary, the assignment mechanism of issuing heat alerts is unknown and needs to be modelled based on observed covariates. We also obtained 4-km gridded estimates of daily maximum temperature and vapor-pressure deficit using the Parameter-elevation Regressions on Independent Slopes Model (PRISM) (Daly et al. 2008, Daly 2013). From these variables, we calculate time series data of population-weighted daily maximum heat index for each county. This approach is described by Spangler et al. (2019) and implemented by the R package by Anderson et al. (2013).

As outcomes, we consider daily all-cause deaths among the entire Medicare enrollees and cause-specific hospitalizations for five heat-related diseases (heat stroke, urinary tract infections, septicemia, renal failure, fluid and electrolyte disorders) using Clinical Classifications Software (CCS) groupings of principal discharge diagnosis codes among the Medicare Fee-for-Service (FFS) enrollees, which have been previously reported in Bobb et al. (2014). Figure 1 presents the geographic distribution of the 2817 U.S. counties with heat index data available. The minimal threshold heat index (i.e., the lowest heat index to trigger a heat alert) of all heat alert days across 2006-2016 for each county is presented in the upper panel, and the number of heat alert days for each county across 2006-2016 is presented in the lower panel. We observe that the minimal threshold heat index tends to be lower in the north; whereas counties in Florida and Texas had the highest threshold heat index. Counties in the south east and south California issued the most heat alerts. Table 1 summarizes the characteristics for NWS-issued heat alerts and our health outcomes. We find that the issuance of heat alerts is rare, that is, it occurs on average in less than 3% of warm season days.

Minimal Threshold Heat Index of All Heat Alert Days across 2006-2016



Number of Heat Alert Days across 2006-2016

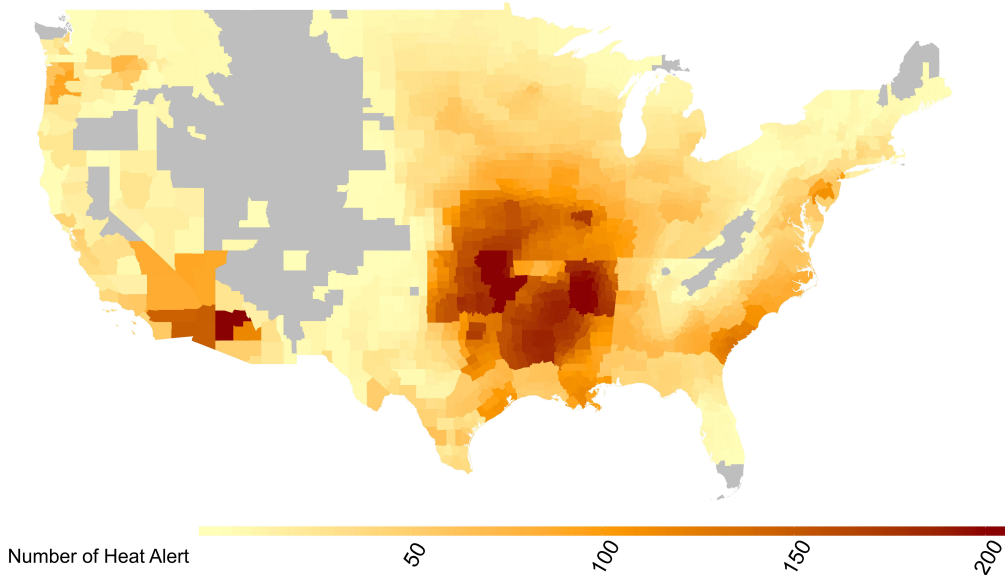


Figure 1: The minimal threshold heat index of all heat alert days per county (upper panel) and the number of heat alerts days per county (lower panel) in all 2817 counties across April-October of 2006-2016. We observe that the minimal threshold heat index tends to be lower in the north; whereas counties in Florida and Texas had the highest threshold heat index. Counties in the south east and south California issued the most heat alerts. Counties in gray represent those counties with insufficient heat alert data, which were excluded from this study.

Table 1: Characteristics for NWS-issued heat alerts, all-cause deaths among Medicare enrollees, and cause-specific hospitalizations for five heat-related diseases among Medicare FFS enrollees across April-October of 2006-2016

Variables	2817 Counties	550 Populous Counties ¹
% Days with Heat Alerts	2.52 %	2.22 %
# of Deaths	10,467,201	7,653,987
# of Heat stroke	97,399	72,649
# of Urinary tract infections	1,424,046	1,061,060
# of Septicemia	2,614,871	1,954,011
# of Renal failure	1,207,903	894,164
# of Fluid and electrolyte disorders	928,270	673,007

1. Counties with population > 100,000.

We focus on the following causal question "If we had changed the odds of issuing heat alerts by δ_t -fold on day t for each day in the warm season, how many deaths would have been averted and how many hospitalizations for heat-related diseases could have been avoided?" One could estimate the total number of deaths and hospitalizations avoided for the entire warm season. Alternatively, there may be interest in estimating the number of deaths and hospitalizations avoided among extremely hot days rather than the entire warm season. We defined "extremely hot days" to be the top 5% hottest days with a heat index that exceeded 95% of warm season days in the corresponding county. We believe deaths and hospitalizations attributable to heat (and avoidable to heat alert) are more likely to happen on extremely hot days, and therefore this quantity may have more policy relevant impact: help us to assess the effectiveness of heat alerts and insights into how to improve them to better protect the public's health from extreme heat events.

Figure 2 illustrates the comparison between the observed frequency of the actual heat alerts and the anticipated heat alerts in one counterfactual setting where the odds of issuing heart alerts were increased by 10-times for each day in the warm season. It is worth clarifying that increasing the odds of issuing a heat alert by 10-times for each day in

NWS-issued heat alerts in Los Angeles county 2006-2016

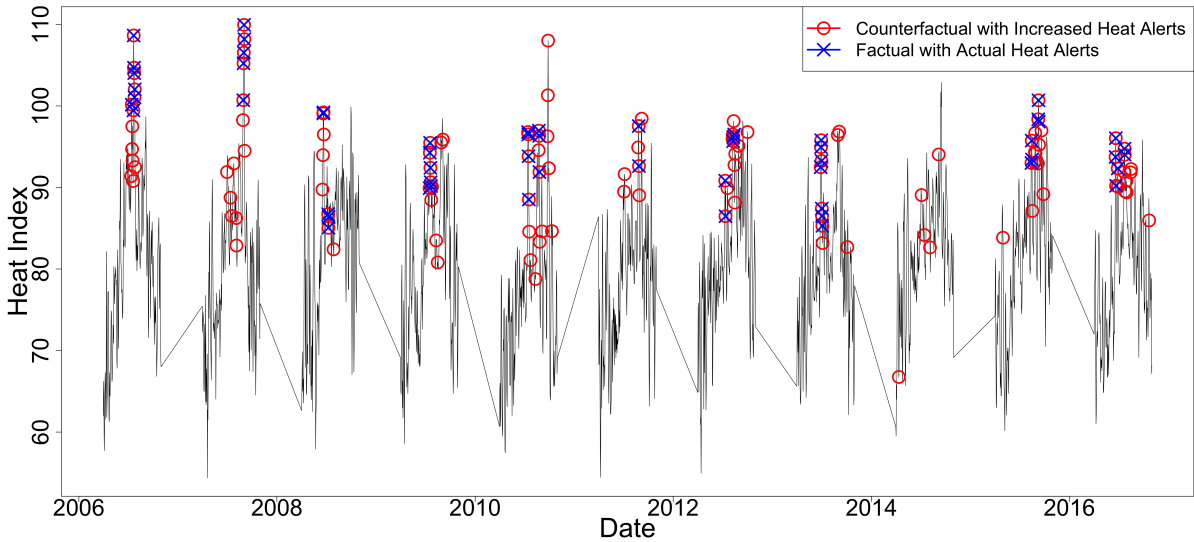


Figure 2: NWS-issued heat alerts for Los Angeles county 2006-2016. The blue x's represent the actual heat alerts that have been issued and the red circles represents the anticipated heat alerts under a counterfactual scenario where the odds of issuing heat alerts were increased by approximately 10-times for every warm season day resulting in approximately 2.3 times as many heat alerts. We find under this counterfactual scenario, Los Angeles county would have experienced 128 heat alerts 2006-2016, compared to the 56 heat alerts that were actually issued.

the warm season is not equivalent to increasing the number of heat alerts by 10-times in total. For example, if the probability of issuing a heat alert on day t is 90%, the probability of issuing a heat alert would increase to $\frac{10 \times 90\%}{10 \times 90\% + 1 - 90\%} \approx 98.9\%$ under the stochastic intervention corresponding to a 10-fold increase in odds. Taking Los Angeles county as an example, we find that if we increase the odds of issuing a heat alert by 10-times on all warm season days, the local NWS office would have issued 128 heat alerts across 2006-2016 under this counterfactual setting, compared to the total of 56 heat alerts that the NWS office actually issued. That is increasing the odds by 10-times results in increasing the heat alerts issued by 2.3-fold from 56 to 128. Notably, under this counterfactual setting,

the heat alerts issued in the real setting would still be issued in warm season days with extreme heat index. In addition to these heat alerts, under the counterfactual setting, heat alerts are more likely to be issued on days with moderate heat index.

3 Methods

3.1 Notations, Intervention and Estimand

In this section, we introduce the notation in the context of time series data (in our motivating example, i is the county). Let $Y_{i,t}, W_{i,t}, C_{i,t}$ be the outcome, treatment and additional covariates at time t , for $t \in \{1, 2, \dots, T\}$ in county i . Because the focus of this section is to introduce the causal estimands for a single time series we omit the index i . In Section 5, we will extend the notation and the methodology to multiple time series.

Each time t can be assigned to the treatment $W_t = 1$ or $W_t = 0$, and subsequently the outcome Y_t is observed. We define $\{C_{1:T} = (C_1, \dots, C_T), W_{1:T} = (W_1, \dots, W_T), Y_{1:T} = (Y_1, \dots, Y_T)\}$. We assume that W_t is binary; Y_t and C_t can be binary, categorical or continuous, in which C_t includes pre-treatment covariates prior to the treatment assignment at time t (e.g., the heat index of day t in our motivating example).

We denote by \mathcal{F}_t the filtration which is used to capture past information prior to the treatment assignment at time t , that is $\mathcal{F}_t = \{C_{1:t}, W_{1:(t-1)}, Y_{1:(t-1)}\}$. Following the potential outcome framework for time series data (Bojinov & Shephard 2019), we denote $Y_t(w_{1:t})$ the potential outcome at time t that would have been observed under treatment path $w_{1:t} = (w_1, \dots, w_t)$, and we introduce the potential outcome path $Y_{1:t}(w_{1:t}) = \{Y_1(w_{1:1}), Y_2(w_{1:2}), \dots, Y_t(w_{1:t})\}$. See Figure 3a as an example of all the potential outcome paths, for $T = 3$. If we assume, $w_{1:3} = (1, 1, 1)$, then the observed outcome path is $\{Y_1(1), Y_2(1, 1), Y_3(1, 1, 1)\}$ (see the bold blue arrows in Figure 3a).

We define the time-varying propensity score at time t as

$$p_t(w_t, \mathcal{F}_t) = Pr(W_t = w_t | \mathcal{F}_t), \text{ for } w_t = \{0, 1\}.$$

In our motivating example, the time-varying propensity score denotes the probability of issuing a heat alert on day t conditional on all past information up to day t just prior to the heat alert issuance.

Following Kennedy (2019), instead of assuming that the intervention is *deterministic*, we assume that the intervention is *stochastic*. An intervention is deterministic if a given day is deterministically assigned to a treatment ($W_t = 1$) or not ($W_t = 0$). An intervention is *stochastic* if a given day t is *randomly* assigned to the treatment based on the incremental propensity score defined as

$$p_t^{\text{Inc}}(w_t = 1, \mathcal{F}_t) := \frac{\delta_t p_t(w_t = 1, \mathcal{F}_t)}{\delta_t p_t(w_t = 1, \mathcal{F}_t) + 1 - p_t(w_t = 1, \mathcal{F}_t)} \quad (1)$$

In other words, we assume that on a given day t , the probability of being assigned to the treatment increases by δ_t -fold conditional on past information prior to the treatment assignment at time t .

We now denote $\delta_{1:T} = \{\delta_1, \delta_2, \dots, \delta_T\}$, the intervention path, that is a sequence of interventions, where at each time t we assume that the odds of being treated increase by δ_t -fold. We denote $w_{1:t}^{\text{Inc}}(\delta_{1:t})$ the post-intervened treatment path under the intervention path $\delta_{1:t}$. Let $\tau_t(\delta_{1:t}) := Y_t(w_{1:t}^{\text{Inc}}(\delta_{1:t}))$, which denotes the potential outcome at time t with respect to the post-intervened treatment path $w_{1:t}^{\text{Inc}}(\delta_{1:t})$, which further depends on the stochastic intervention path $\delta_{1:t}$. Figure 3 provides an example where $\delta_{1:3} = \{2, 2, 2\}$, that is for three consecutive days, we increase the odds of receiving the treatment by 2-fold (for simplicity we consider a common δ across the three days, but in practice these could vary). Figure 3**b** represents the causal relationship between treatment path $W_{1:T} = (W_1, \dots, W_T)$, covariate path $\{C_{1:T} = (C_1, \dots, C_T)\}$, and potential outcome path $Y_{1:T} = (Y_1, \dots, Y_T)\}$ pre-intervention. The proportions of blue shading reflect the probabilities of receiving the treatment on each day, that are $p_1(w_1 = 1, \mathcal{F}_1) = \frac{1}{4}$ on day 1, $p_2(w_2 = 1, \mathcal{F}_2) = \frac{1}{2}$ on day 2, and $p_3(w_3 = 1, \mathcal{F}_3) = \frac{4}{5}$ on day 3. Figure 3**c** represents the counterfactual time series after the proposed stochastic intervention, in which the probabilities of receiving the treatment increase due to the sequence of proposed stochastic interventions $\delta_{1:3} = \{2, 2, 2\}$. After the interventions $\delta_{1:3} = \{2, 2, 2\}$, the probability of receiving the treatment $W_1 = 1$ on day 1 in-

creases to $p_1^{\text{Inc}}(w_1 = 1, \mathcal{F}_1) = \frac{2 \times p_1(w_1=1, \mathcal{F}_1)}{2 \times p_1(w_1=1, \mathcal{F}_1) + 1 - p_1(w_1=1, \mathcal{F}_1)} = \frac{2}{5}$; similarly, $p_2^{\text{Inc}}(w_2 = 1, \mathcal{F}_2) = \frac{2}{3}$ and $p_3^{\text{Inc}}(w_3 = 1, \mathcal{F}_3) = \frac{8}{9}$.

Unlike the common causal estimands which are generally defined as averages of subject level potential outcomes, here we define the causal estimand on a set of potential outcomes in correspondence of a given intervention path. In our context, we define the causal estimand as the temporal average of the potential outcomes up to time T ,

$$\bar{\tau}(\delta_{1:t,T}) = \frac{1}{T} \sum_{t=1}^T \tau_t(\delta_{1:t})$$

This causal estimand can be explained as the average of potential outcome during the time period up to T , had the odds of receiving treatment increased by δ_t -fold for each day $t = 1, \dots, T$. In our motivating example, the temporal average of the potential outcomes represents the daily average deaths or hospitalizations in a county had the odds of receiving treatment increased by δ_t -fold on day t for each day within a warm season. Moreover, analog to the conditional average causal estimand (CATE), we can calculate the average of deaths or hospitalizations over days with pre-specified conditions (e.g., extremely hot days).

We also introduce another causal estimand which is the summation of potential outcomes during the time period up to T . This causal estimand characterizes the total number of deaths or hospitalizations in a county, had the odds of receiving treatment increased by δ_t -fold on day t .

3.2 Causal Estimand on Observed Treatment Path

There are major limitations that are associated with the causal estimands $\bar{\tau}(\delta_{1:T})$ defined in Section 3.1: First, $\tau_T(\delta_{1:T})$ depends on a treatment path that the length increases throughout time T , thus one needs to impose stringent modelling assumptions to extrapolate its values; Second, the asymptotic theory for these causal estimands is hard to establish as T goes to infinity, because $\tau_T(\delta_{1:T})$ depends on an infinite set of variables. Motivated by Bojinov & Shephard (2019), we define a t_0 -step causal estimand conditional on the observed treatment path $w_{1:(t-t_0)}^{obs}$ named $\tau_t(\delta_{(t-t_0+1):t})$ and its temporal average counterpart

named $\bar{\tau}(\delta_{(t-t_0+1):t,T})$, that are

$$\begin{aligned}\tau_t(\delta_{(t-t_0+1):t}) &= Y_t(w_{1:(t-t_0)}^{obs}, w_{(t-t_0+1):t}^{\text{Inc}}(\delta_{(t-t_0+1):t})), \quad t_0 = 1, 2, \dots, t-1 \\ \bar{\tau}(\delta_{(t-t_0+1):t,T}) &= \frac{1}{T-t_0+1} \sum_{t=t_0}^T \{\tau_t(\delta_{(t-t_0+1):t})\}.\end{aligned}$$

By making the estimands dependent on the observed treatment path $w_{1:(t-t_0)}^{obs}$, we define causal estimands that can be estimated nonparametrically (see in Section 4). The use of t_0 -step causal estimands are consistent with time series models with pre-specified fixed memory (e.g., Autoregressive integrated moving average (ARIMA) model). They are also compatible with the causal inference literature since they can be treated as conditional causal estimands condition on partial historical information $\{W_{1:(t-t_0)} = w_{1:(t-t_0)}^{obs}\}$ (Imbens & Rubin 2015). We can also establish a central limit theorem about the t_0 -step causal estimator with respect to $T \rightarrow \infty$ (see Section 4).

Besides the theoretical convenience described above, the use of t_0 -step causal estimands has important practical implications. In our motivating example, we may assume that death or hospitalization risks for today don't depend on heat alerts issued many days before as heat alerts deliver instant information about extreme heat events to the public, and thus their effects are expected to last a very short period of time.

3.3 Assumptions and Identification

Following the potential outcomes framework (Rubin 1974) adapted to the time-varying treatment regime (Robins et al. 2000), we establish the following assumptions of causal identification:

Assumption 1 (SUTVA) *The potential outcomes are non-anticipating, and consistent, that is $Y_t^{obs} = Y_t(w_{1:T}^{obs}) = Y_t(w_{1:t}^{obs}) \forall t = 1, \dots, T$.*

Assumption 1 generalizes the usual Stable Unit Treatment Value (SUTVA) assumption (Imbens & Rubin 2015) to allow for the potential outcome at time t to depend on the whole path of past treatment assignments, yet not to be affected by future treatment assignments

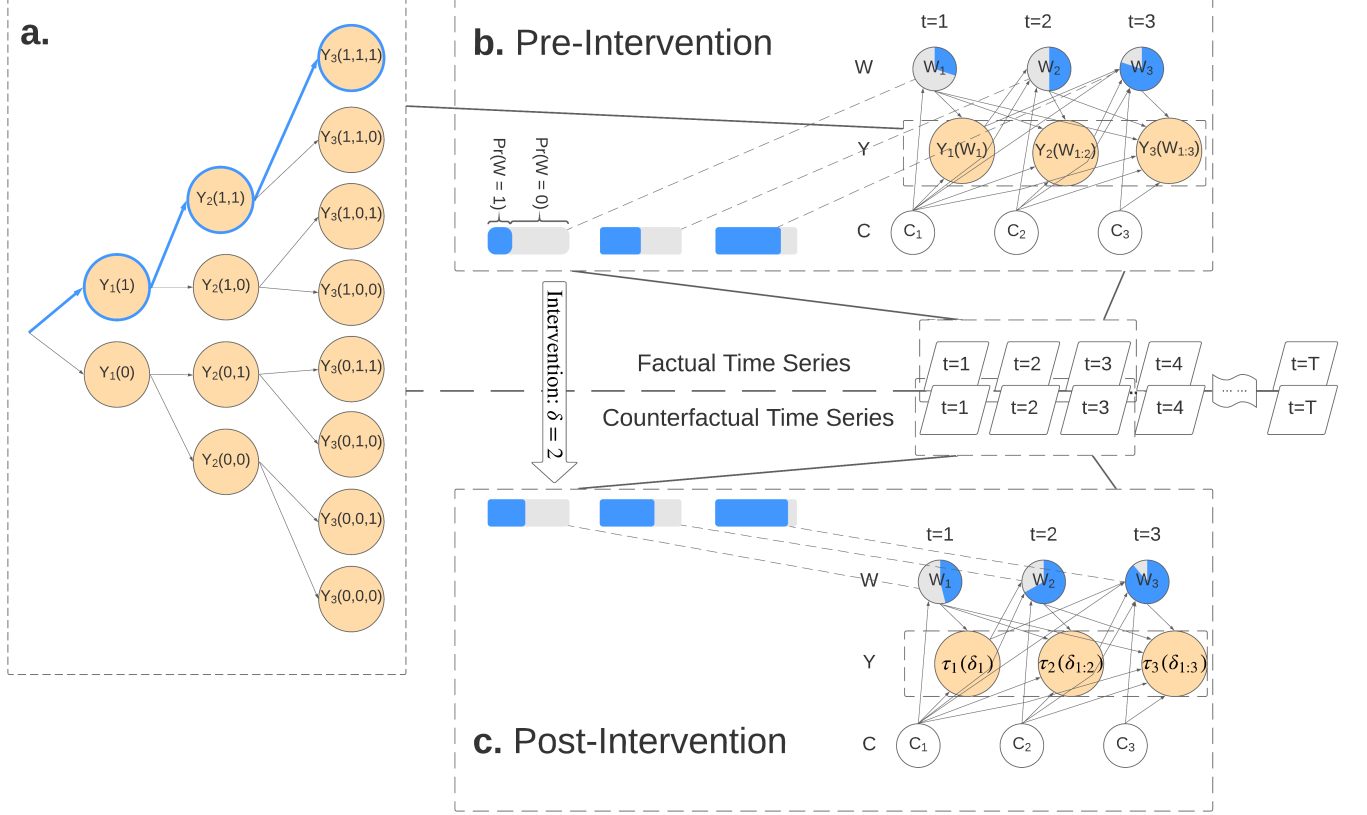


Figure 3: Overview of notation, intervention and estimand of one time series. $\delta_{1:3} = \{2, 2, 2\}$, that is we increase the odds of receiving treatments by 2-fold for each day $t = 1, 2, 3..$ **a.** We illustrate all the potential outcome paths for $T = 3$. The blue lines and circles represents the potential outcome path $\{Y(w_1), Y_2(w_{1:2}), Y_3(w_{1:3})\}$ given the treatment path $W_{1:3} = w_{1:3} = (1, 1, 1)$. **b.** The causal relationship between treatment path $W_{1:T} = (W_1, \dots, W_T)$, covariate path $C_{1:T} = (C_1, \dots, C_T)$, and potential outcome path $Y_{1:T} = (Y_1, \dots, Y_T)$ pre-intervention. The proportions of blue shading reflect the probabilities of receiving treatments at each day, that are $p_1(w_1 = 1, \mathcal{F}_1) = \frac{1}{4}$ on day 1, $p_2(w_2 = 1, \mathcal{F}_2) = \frac{1}{2}$ on day 2, and $p_3(w_3 = 1, \mathcal{F}_3) = \frac{4}{5}$ on day 3. **c.** The counterfactual time series with outcome path $\{\tau_1(\delta_1) = Y(w_1^{\text{Inc}}(\delta_1)), \tau_2(\delta_{1:2}) = Y_2(w_{1:2}^{\text{Inc}}(\delta_{1:2})), \tau_3(\delta_{1:3}) = Y_3(w_{1:3}^{\text{Inc}}(\delta_{1:3}))\}$ after the proposed stochastic intervention $\delta_{1:3}$, in which the probabilities of receiving treatments altered. The probability of receiving the treatment $W_1 = 1$ on day 1 increases to $p_1^{\text{Inc}}(w_1 = 1, \mathcal{F}_1) = \frac{2 \times p_1(w_1 = 1, \mathcal{F}_1)}{2 \times p_1(w_1 = 1, \mathcal{F}_1) + 1 - p_1(w_1 = 1, \mathcal{F}_1)} = \frac{2}{5}$; similarly, $p_2^{\text{Inc}}(w_2 = 1, \mathcal{F}_2) = \frac{2}{3}$ and $p_3^{\text{Inc}}(w_3 = 1, \mathcal{F}_3) = \frac{8}{9}$.

(non-anticipating). We still assume that there is only one version of the treatment for each time t , and each treatment path up to time t realizes a unique observed outcome at time t (consistency).

Assumption 2 (Unconfoundedness) *The assignment mechanism is unconfounded if for all $W_{1:T} \in \mathcal{W} = \{0, 1\}^T$, $W_t \perp Y_s(w_{1:s}) \mid \mathcal{F}_t \forall t = 1, \dots, T$ and $t \leq s \leq T$.*

Assumption 2 aligns with the "sequential randomization" assumption introduced in longitudinal studies by Robins et al. (1994), which states that the treatment assignment only depends on the past information and thus is conditionally independent of future potential outcomes. This assumption also excludes the possibility that future potential outcomes could impact the current treatment assignment retrospectively (a phenomenon which has been discussed in Granger (1980)).

Assumption 3 (Weak overlap) *The assignment mechanism weakly overlaps if for all $t \in \{1, 2, \dots, T\}$,*

$$p_t(w_t \mid \mathcal{F}_t) = 0 \Rightarrow p_t^{Inc}(w_t \mid \mathcal{F}_t) = 0$$

The usual overlap assumption in the standard deterministic intervention requires that the assignment at each time $t \in \{1, 2, \dots, T\}$ has a positive probability of assigning each treatment conditional on the filtration \mathcal{F}_t . On the other hand, the proposed stochastic intervention framework avoids the usual overlap assumption (Kennedy 2019) by not intervening at time points which have zero probabilities of receiving certain treatment conditions. Noting that the stochastic intervention described in Section 3.1 always meets the weak overlap assumption, since $p_t^{Inc}(w_t \mid \mathcal{F}_t) = 0$ always holds when the propensity $p_t(w_t \mid \mathcal{F}_t) = 0$ no matter the value of δ_t .

We show the identification of the proposed causal estimand under the SUTVA, unconfoundedness and the weak overlap assumptions. At any time point $t \in \{1, \dots, T\}$, $\tau_t(\delta_{1:t})$ can be defined as

$$\tau_t(\delta_{1:t}) = \sum_{w_{1:t} \in W_{1:t}} \int_{\partial\mathcal{F}_{1:t}} \mu(\mathcal{F}_t) \times \prod_{s=1}^t \underbrace{\frac{[w_s \delta_s p_s(1, \mathcal{F}_s) + (1 - w_s)p_s(0, \mathcal{F}_s)]}{\delta_s p_s(1, \mathcal{F}_s) + 1 - p_s(1, \mathcal{F}_s)}}_{:= p_s^{Inc}(w_s \mid \mathcal{F}_s)} \times dPr(\partial\mathcal{F}_s \mid \mathcal{F}_{s-1})$$

where $\partial\mathcal{F}_{1:t} = \partial\mathcal{F}_1 \times \dots \times \partial\mathcal{F}_t$, $\partial\mathcal{F}_s = \mathcal{F}_s/\mathcal{F}_{s-1}$, $s = 1, \dots, t$, and $\mu(\mathcal{F}_t) = E(Y_t \mid W_t, \mathcal{F}_t)$. It is worth noting that although $\tau_t(\delta)$ is causally identifiable, the corresponding quantity may be practically infeasible to estimate using a single time series. We instead focus on the temporal average causal estimand

$$\bar{\tau}(\delta_{1:t,T}) = \frac{1}{T} \sum_{t=1}^T \tau_t(\delta_{1:t}),$$

which can also be causally identified given $\tau_t(\delta_{1:t})$ is identifiable $\forall t = 1, 2, \dots, T$. Likewise, the t_0 -step causal estimand $\tau_t(\delta_{(t-t_0+1):t})$ and its temporal average counterpart $\bar{\tau}(\delta_{(t-t_0+1):T})$ can be identified under the same assumptions.

4 Estimation and Inference

We focus on the estimation and inference of t_0 -step causal estimands given the theoretical and practical conveniences stated in Section 3.2. To estimate the proposed causal estimands, we propose the following estimator based on time-varying propensity scores. If the time-varying propensity score $p_s(w_s, \mathcal{F}_s)$ is known, as in Section 6 of Kim et al. (2019), we can have an unbiased estimator for a t_0 -step estimand on observed treatment path $\tau_t(\delta_{(t-t_0+1):t})$ defined as,

$$\hat{\tau}_t(\delta_{(t-t_0+1):t}) = \prod_{s=t-t_0+1}^t \underbrace{\left\{ \frac{[W_s \delta + (1 - W_s)]}{\delta p_s(1, \mathcal{F}_s) + 1 - p_s(1, \mathcal{F}_s)} \right\}}_{:= p^{\text{Inc}}_s(w_s | \mathcal{F}_s)} Y_t$$

When the time-varying propensity score $p_s(w_s, \mathcal{F}_s)$ is unknown, the estimation strategy requires two steps. First, at each time point s , we need to estimate the time-varying propensity score $\hat{p}_s(w_s, \mathcal{F}_s)$. Second, if the propensity scores can be modeled with correct model specifications, we can construct the following unbiased estimator for a t_0 -step

estimand on observed treatment path.

$$\hat{\tau}_t(\delta_{(t-t_0+1):t}) = \prod_{s=t-t_0+1}^t \underbrace{\left\{ \frac{[W_s \delta + (1 - W_s)]}{\delta \hat{p}_s(1, \mathcal{F}_s) + 1 - \hat{p}_s(1, \mathcal{F}_s)} \right\} Y_t}_{:= \widehat{p}^{\text{Inc}}_s(w_s | \mathcal{F}_s)}$$

$$\hat{\tau}(\delta_{(t-t_0+1):t,T}) = \frac{1}{T-t_0+1} \sum_{t=t_0}^T \hat{\tau}_t(\delta_{(t-t_0+1):t}) = \frac{1}{T-t_0+1} \sum_{t=t_0}^T \left\{ \prod_{s=t-t_0+1}^t \left\{ \frac{[W_s \delta + (1 - W_s)]}{\delta \hat{p}_s(1, \mathcal{F}_s) + 1 - \hat{p}_s(1, \mathcal{F}_s)} \right\} Y_t \right\}$$

One important feature of the proposed estimator is that the temporal observed outcomes are weighted by a time-varying weights which correspond to the product of estimated incremental propensity scores $\widehat{p}^{\text{Inc}}_s(w_s | \mathcal{F}_s)$.

4.1 Variance Estimator

Given the proposed estimator, we calculate the variance estimator for $\hat{\tau}_t(\delta_{(t-t_0+1):t})$,

$$\Sigma_t(\delta_{(t-t_0+1):t}) = E \left\{ \underbrace{\prod_{s=t-t_0+1}^t \left(\frac{[W_s \delta_s + (1 - W_s)]}{\delta \hat{p}_s(1, \mathcal{F}_s) + 1 - \hat{p}_s(1, \mathcal{F}_s)} \right)^2 Y_t^2}_{\mathcal{V}} \right\}$$

$$- \left\{ E \left[\prod_{s=t-t_0+1}^t \left(\frac{[W_s \delta_s + (1 - W_s)]}{\delta \hat{p}_s(1, \mathcal{F}_s) + 1 - \hat{p}_s(1, \mathcal{F}_s)} \right) Y_t \right] \right\}^2$$

In which

$$\mathcal{V} = \sum_{w_{(t-t_0+1):t} \in W_{(t-t_0+1):t}} \int_{\partial \mathcal{F}_{(t-t_0+1):t}} E(Y_t^2 | W_{(t-t_0+1):t} = w_{(t-t_0+1):t}, \mathcal{F}_t) \times$$

$$\prod_{s=(t-t_0+1)}^t \underbrace{\left\{ \frac{[w_s \delta_s p_s(1, \mathcal{F}_s) + (1 - w_s) p_s(0, \mathcal{F}_s)]}{\delta_s p_s(1, \mathcal{F}_s) + 1 - p_s(1, \mathcal{F}_s)} \right\}^2}_{:= p_s^{\text{Inc}}(w_s | \mathcal{F}_s)^2} \times dPr(\partial \mathcal{F}_s | \mathcal{F}_{s-1})$$

$$\hat{\mathcal{V}} = \prod_{s=t-t_0+1}^t \left\{ \frac{[W_s \delta_s^2 + (1 - W_s)]}{[\delta_s \hat{p}_s(1, \mathcal{F}_s) + 1 - \hat{p}_s(1, \mathcal{F}_s)]^2} \right\} Y_t^2$$

4.2 Asymptotic Theory

We then establish the asymptotic properties of the proposed estimators on one time series with respect to time T . Using martingale theory show in Bojinov & Shephard (2019), we

show the proposed estimators are \sqrt{T} -asymptotically normal.

Theorem 1 (Asymptotic Normal) *If Assumptions 1–3 hold, and there exist*

$$\frac{1}{T - t_0 + 1} \sum_{t=t_0}^T \hat{\Sigma}_t(\delta_{(t-t_0+1):t}) \longrightarrow \Sigma,$$

as $T \rightarrow \infty$. We have,

$$\begin{aligned} \sqrt{T} \left[\frac{1}{T - t_0 + 1} \hat{\tau}_t(\delta_{\{(t-t_0+1):t,T\}}) - \frac{1}{T - t_0 + 1} \bar{\tau}_t(\delta_{\{(t-t_0+1):t,T\}}) \right] \\ \longrightarrow N(0, \Sigma) \end{aligned}$$

5 Meta-analysis on Multiple Time Series

In many applications including our motivating example, we have a number of counties with their distinct time series. To combine information across counties, we generalize our stochastic intervention framework to the context of meta-analysis of heterogeneous time series. To formalize the causal identification in the context of multiple time series, we introduce and discuss new assumptions of identification in Section 5.1. In subsequent Section 5.2, we describe estimation and inference of the pooled estimator based on meta-analysis models.

5.1 Assumptions and Identification

Before we formally introduce the new pooled estimator, additional assumptions are needed to allow causal inference from multiple time series. We introduce the subscript i to denote the subject, that is, the county in our motivating application.

Assumption 4 (Multiple Subject SUTVA) *The potential outcomes are non-anticipating, non-interfering, and consistency, that is $Y_{i,t}^{obs} = Y_{i,t}(w_{1:N,1:T}^{obs}) = Y_{i,t}(w_{1:N,1:t}^{obs}) = Y_{i,t}(w_{i,1:t}^{obs}) \forall i = 1, \dots, N; t = 1, \dots, T$.*

Assumption 4 generalizes Assumption 1 under multiple subjects settings. A notable constraint, beyond the non-anticipating and consistency which were held in Assumption 1, is that the potential outcomes for a subject are only affected by their own treatment path, yet not to be affected by spillover effects across other subjects (non-interfering).

Assumption 5 (Multiple Subject Unconfoundedness) *The assignment mechanism is unconfounded if for all $W_{i,1:T} \in \mathcal{W} = \{0, 1\}^T$, and $\mathcal{F}_t = \{\mathcal{F}_{1,t}, \dots, \mathcal{F}_{N,t}\}$, then $W_{i,t} \perp Y_{i,s}(w_{i,1:s}) \mid \mathcal{F}_t \forall i = 1, \dots, N; t = 1, \dots, T$ and $t \leq s \leq T$.*

Assumption 5 is similar to Assumption 2, which still states the treatment path for each subject only depends on the past information, yet it does not rule out the possibility that the propensity of one subject is treated at time t would reply on the confounders, treatment, or outcome of another subject before the treatment assignment at time t . There is no need to assume that the potential outcome of subject i , $Y_{i,1:t}(w_{i,1:t})$ is independent with the potential outcome of subject j , $Y_{j,1:t}(w_{j,1:t})$ for $i \neq j$.

Assumption 6 (Random Effects under Identical Intervention Path) *The intervention path $\delta_{1:T}$ is identical across multiple time series. The t_0 -step causal estimand $\bar{\tau}_i(\delta_{(t-t_0+1):t})$ under the intervention path $\delta_{1:T}$ are independent across $i = 1, \dots, N$, $\forall t = 1, \dots, T; t_0 = 1, \dots, t$.*

Assumption 6 is the assumption needed for random-effect meta-analysis. Although the intervention paths $\delta_{i,1:T}, i \in \{1, 2, \dots, N\}$ do not have to be the same for every subject i , in a meta-analysis settings, it is more practically meaningful to assume the same intervention path $\delta_{1:T}$ across all subjects. Importantly, Assumption 6 sets no constraint on the observed treatment path $W_{i,1:T}, i \in \{1, 2, \dots, N\}$, which can be distinct for each subjects. Under the random-effects meta-analysis framework we allow the true causal estimands to differ for different subjects, yet to represent a random sample from a particular distribution.

Here we create a weighted average causal estimand across N units, as

$$\bar{\tau}^N(\delta_{(t-t_0+1):t,T}) = \sum_{i=1}^N c_i \bar{\tau}_i(\delta_{(t-t_0+1):t,T}),$$

where $\sum_{i=1}^N c_i = 1$ and $\{c_i, i = 1, 2, \dots, N\}$ are fixed.

When Assumption 4-6 hold, we show $\bar{\tau}^N(\delta_{(t-t_0+1):t,T})$ are causally identified using a modified version of identification equation from Section 3, that is, $\forall i \in \{1, 2, \dots, N\}$

$$\begin{aligned}\tau_{i,t}(\delta_{1:t}) &= \sum_{w_{i,1:t} \in W_{i,1:t}} \int_{\partial\mathcal{F}_{1:t}} \mu(\mathcal{F}_t) \times \prod_{s=t-t_0+1}^t \underbrace{\frac{[w_{i,s} \delta_s p_{i,s}(1, \mathcal{F}_{i,s}) + (1 - w_{i,s}) p_{i,s}(0, \mathcal{F}_s)]}{\delta_s p_{i,s}(\mathcal{F}_s) + 1 - p_{i,s}(\mathcal{F}_s)}}_{:= p_{i,s}^{\text{Inc}}(w_{i,s} | \mathcal{F}_s)} \times dPr(\partial\mathcal{F}_s | \mathcal{F}_{s-1}), \\ \bar{\tau}_i(\delta_{(t-t_0+1):t,T}) &= \frac{1}{T - t_0 + 1} \sum_{t=t_0}^T \tau_{i,t}(\delta_{(t-t_0+1):t}), \\ \bar{\tau}^N(\delta_{(t-t_0+1):t,T}) &= \sum_{i=1}^N c_i \bar{\tau}_i(\delta_{(t-t_0+1):t,T}).\end{aligned}$$

where $\partial\mathcal{F}_{1:t} = \partial\mathcal{F}_1 \times \dots \times \partial\mathcal{F}_t$, and $\partial\mathcal{F}_s = \mathcal{F}_s / \mathcal{F}_{s-1}, s = 1, \dots, t$, $\mu(\mathcal{F}_t) = E(Y_t | W_t, \mathcal{F}_t)$. $\{c_i, i = 1, 2, \dots, N\}$ are the fixed weights satisfying $\sum_{i=1}^N c_i = 1$. The remaining question is how to choose suitable weights c_i for each subject i .

5.2 Estimation and Inference

There are at least two popular statistical models for meta-analysis, the fixed-effect model and the random-effects model (Borenstein et al. 2010). In general, we found the random-effects assumption is more plausible in our motivating example, given there is generally no reason to assume that the causal effects of heat alerts on health outcomes are identical across all counties. We propose meta-analysis methods relying on random-effects models to obtain a pooled estimator that summarizes the causal effects obtained by time series data across multiple counties (Serghiou & Goodman 2019).

In meta-analysis, for the purpose of obtaining a weighted average causal estimand that characterizes the causal effect obtained by multiple studies (i.e., counties), we want to

assign more weight to studies that yield a more precise estimate of that effect. Under random-effects model, there are two sources of variance (Borenstein et al. 2010). First, the observed causal effect $\hat{\tau}_i(\delta_{(t-t_0+1):t,T})$ for any time series differs from that time series's true effect because of within-study error variance, V_i . Second, the true effect from each time series differs from the weighted average causal effect because of between-study variance. Therefore, the weight assigned to each time series under the inverse variance scheme is

$$c_i = \frac{1}{V_i + \tau^2}, \quad i = 1, 2, \dots, N$$

Note that the within-study error variance, V_i , is unique to each time series, but the between-study variance τ^2 is common to all time series.

6 Simulation Study

We study finite-sample properties of the proposed estimators via simulation study on a single time series, in which we vary: a) the length of the time series T ; b) the step size of the estimator t_0 ; and c) the assignment mechanisms of the treatment $p_t(W_t = 1 | \mathcal{F}_t)$. To reflect the nature of treatment assignment in our motivation example, we generate the treatment W_t under a non-overlap setting (i.e., in general, more than 80% of time t with $p_t(W_t = 1 | \mathcal{F}_t) > 0.9$ or $p_t(W_t = 1 | \mathcal{F}_t) < 0.1$). In particular, we consider a time series with length T . For each $t = 1, \dots, T$,

$$\begin{aligned} \mathbf{C}_t &= (C_{1,t}, C_{2,t}, C_{3,t}, C_{4,t}, C_{5,t}) \sim N(\mathbf{0}, \mathbf{I}_5) \\ p_t(W_t = 1 | \mathcal{F}_t) &= \text{expit}(10 \times \mathbf{C}_t - W_{t-1} + 0.5) \\ Y_t | W_t, W_{t-1}, \mathbf{C}_t &\sim N(3 \times W_t + W_{t-1} + C_{1,t} + C_{2,t} + C_{3,t} + C_{4,t} + C_{5,t}, 1) \end{aligned}$$

At time t , the assignment mechanism of the treatment W_t is stochastic and depends on both \mathbf{C}_t , and the treatment at time $t - 1$, W_{t-1} . Also please note that the outcome Y_t is affected by the treatments both at time t and $t - 1$. The main quantity of interest is the t_0 -step causal estimand on observed treatment path. We assess the performance of each

estimator by calculating the integrated bias and root mean squared error (RMSE)

$$\begin{aligned}\text{Integrated Bias} &= \frac{1}{J} \sum_{j=1}^J \left| \frac{1}{I} \sum_{i=1}^I \hat{\tau}_i(\delta_{t-t_0+1:t,T,j}) - \bar{\tau}_i(\delta_{t-t_0+1:t,T,j}) \right| \\ \widehat{\text{RMSE}} &= \frac{\sqrt{N}}{J} \sum_{j=1}^J \left[\frac{1}{I} \sum_{i=1}^I (\hat{\tau}_i(\delta_{t-t_0+1:t,T,j}) - \bar{\tau}_i(\delta_{t-t_0+1:t,T,j}))^2 \right]^{1/2}\end{aligned}$$

where $\bar{\tau}(\delta_{t-t_0+1:t,T,j}) := \frac{1}{T-t_0+1} \sum_{t=t_0}^T \bar{\tau}(\delta_{t-t_0+1:t,j})$ is temporal average causal quantity, and $\hat{\tau}(\delta_j)$ is its estimator based on time-varying propensity score. We assess the performances at $J = 50$ values of δ_j equally spaced between 0.1 to 10 across $I = 500$ simulations.

We vary the following combination of (T, t_0) , $T = (200, 1000, 5000)$, and $t_0 = (2, 5, 10)$. We apply two methods to estimate the time-varying propensity scores, 1) logistic regression; 2) Super Learner (Van der Laan et al. 2007), which combines multivariate adaptive regression splines, generalized additive model, generalized linear model, random forest, and recursive partitioning regression trees models. We assume that the form of the propensity score model is correctly specified as $W_t | \mathbf{C}_t, W_{t-1}$. We conduct additional simulations in the Supplementary Materials to show the results when the form of the propensity score model is misspecified.

Table 2 shows the proposed estimator performed well in various settings. Under the same step t_0 , we observed that the integrated bias and RMSE of the estimator decrease when the length of time series T increase, regardless of the time-varying propensity score is estimated by logistic regression or Super Learner. This performance is expected since we have established a central limit theorem with respect to time T . We also observed a decreased performance of the estimator as the step t_0 increases. This phenomenon is not surprising, since the weights in the proposed estimator is defined as the product of t_0 terms of estimated incremental propensity scores. We, in general, expect the absolute bias and RMSE will likely be larger as more estimated product terms are included in the estimator. Noting that in our simulation setting, the outcome Y_t only depends on the treatment of W_t and W_{t-1} , thus causal estimator with $t_0 = 2$ could sufficiently characterize the causal relationship between time series Y_t and $W_t, t \in \{1, 2, \dots, T\}$. We also considered

Table 2: Simulation results for the scenario assuming the time-varying propensity score model is specified with a **logit** link. The Integrated Bias and RMSE (multiplied by 10 for easier interpretation).

T	t_0	Logistic	Super Learner
200	2	0.85 (1.17)	0.66 (1.02)
200	5	1.78 (2.12)	1.26 (1.67)
200	10	3.12 (3.45)	2.30 (2.71)
1000	2	0.36 (0.51)	0.18 (0.38)
1000	5	0.67 (0.79)	0.36 (0.51)
1000	10	1.35 (1.43)	0.79 (0.89)
5000	2	0.11 (0.19)	0.03 (0.16)
5000	5	0.21 (0.28)	0.09 (0.19)
5000	10	0.42 (0.47)	0.16 (0.29)

the hypothetical scenarios of $t_0 = 5$ and $t_0 = 10$ since in data applications, the exact step size t_0 is unknown, thus one can only choose t_0 based on substantive knowledge. The simulation results suggest the choices of t_0 should be parsimonious, that is, choosing a step size t_0 that is capable to capture the data complexity yet is as small as possible to achieve the better performances. We also found that using Super Learner model to estimate the time-varying propensity score leads to improved performances compared to the logistic regression model even if the propensity score model is correctly specified with a **logit** link. This finding suggests that the Super Learner as an ensemble of flexible parametric/non-parametric models are competent in various settings, and additional simulations in the Supplementary Materials indicate promising performances of the Super Learner when the underlying data generating mechanism is unknown and potentially complex.

Figure 4 further shows the curve of 2-step causal effects when the odds of treatment assignment were multiplied by factor $\delta \in [\exp(-2.3), \exp(2.3)]$. The red solid line represents the estimated causal effects along with point-wise 95% point-wise confidence bands

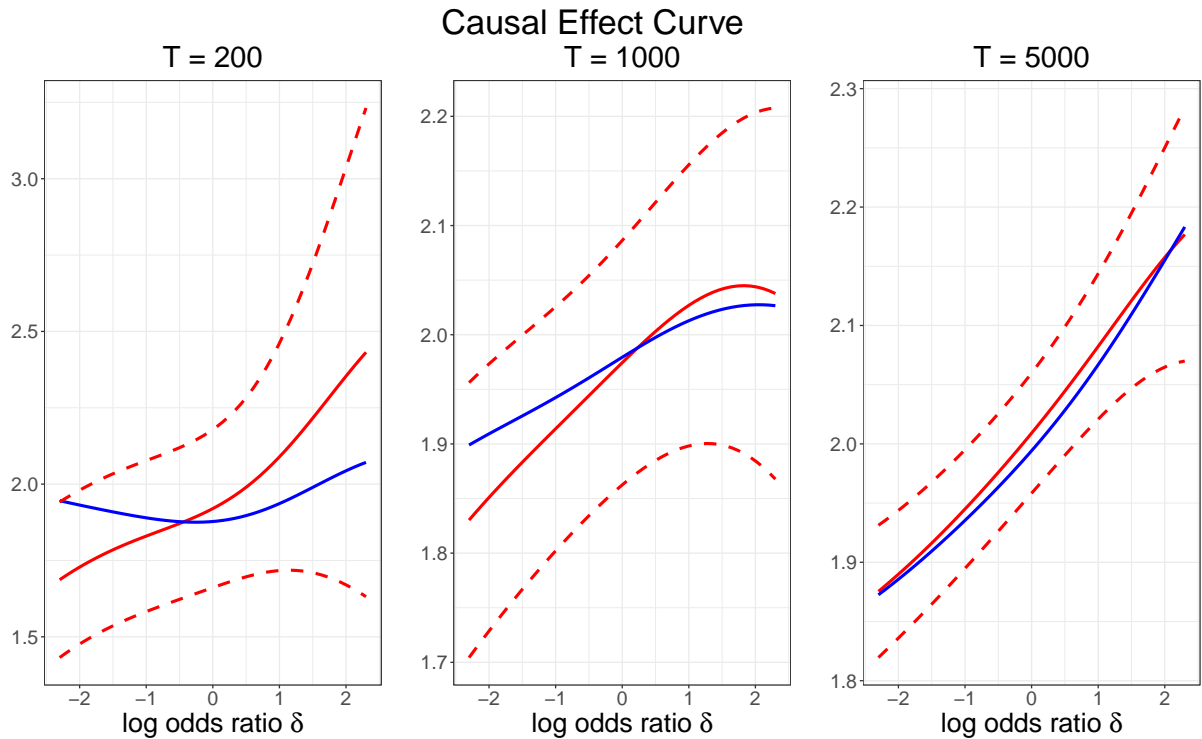


Figure 4: The curve of 2-step causal effects when the odds of treatment assignment were multiplied by factor $\delta \in [\exp(-2.3), \exp(2.3)]$. The red solid line represents the estimated causal effects along with point-wise 95% point-wise confidence bands (red dashed line). The blue solid line represents the true causal effects. The left, middle and right panels reflect the simulation scenarios with $T = 200, 1000, 5000$. The propensity scores were estimated by Super Learner.

(red dashed line). We found that the estimated curve approach the true curve quite well, with improved performances when T increases. The point-wise 95% point-wise confidence bands correctly capture the true curve in all three scenarios with different number of time period $T = 200, 1000, 5000$. We found, in all scenarios, the estimated causal effect curves provided by our proposed approach can capture the true curve accurately, with improved performances when T gets larger. Importantly, the 95% point-wise confidence bands capture the true curve in all settings, showing the proposed variance estimator also perform reasonably well in the simulation study.

7 Application

We analyze the real data described in Section 2. First, we implement the methods proposed in Section 3 to estimate the stochastic causal estimands $\bar{\tau}_i(\delta_{(t-t_0+1):t,T})$ based on the daily time series among warm season days for the years 2006 to 2016 in each county i for $\delta_t \in [\exp(-2.3), \exp(2.3)]$. Returning to our earlier example in Section 2, we assume that absent of the intervention, the probability of issuing a heat alert on day t in county i is 90%. Under a 10-fold increase in odds, that probability would become $\frac{10 \times 90\%}{10 \times 90\% + 1 - 90\%} \approx 98.9\%$. Whereas under 10-fold decrease in odds, the probability would become $\frac{0.1 \times 90\%}{0.1 \times 90\% + 1 - 90\%} \approx 47.4\%$. We assume the same intervention δ for different times t .

In the time-varying propensity score model, we included the following observed covariates: daily maximum heat index, lagged-1 day heat index, lagged-2 day heat index, moving average heat index during this warm season, lagged-1 day heat alert, lagged-2 day heat alert, running total number of heat alerts that have been issued during the corresponding warm season, moving average number of deaths/hospitalizations during the corresponding warm season, and an indicator for holidays.

For each county, we estimate the counterfactual daily all-cause death counts and cause-specific hospitalizations counts for five heat-related diseases (heat stroke, urinary tract infections, septicemia, renal failure, fluid and electrolyte disorders) under several hypothetical scenarios ranging from reducing the odds of issuing heart alerts by 10-times (i.e.,

$\exp(-2.3)$) to increasing the odds by 10-times (i.e., $\exp(2.3)$). We consider the causal estimands with step $t_0 = 3$ as we assume the issuance of heat alerts is unlikely to affect the outcome three or more days later. We define the county-specific causal effect curve for county i as $\bar{\tau}_i(\delta_{(t-2):t,T}) - \bar{\tau}_i(1, 1, 1)$, where $\bar{\tau}_i(\delta_{(t-2):t,T})$ denotes the estimated counterfactual counts under various stochastic interventions ($\delta \in [\exp(-2.3), \exp(2.3)]$) and $\bar{\tau}_i(1, 1, 1)$ denotes the same quantity for a baseline scenario ($\delta = 1$). After obtaining all 2817 county-specific causal effect curves, we utilize the meta-analysis approach proposed in Section 5 to pool the estimated county-specific causal effect curves across counties resulting in the estimation of the pooled causal effect curve, $\sum_{i=1}^N c_i[\bar{\tau}_i(\delta_{(t-2):t,T}) - \bar{\tau}_i(1, 1, 1)]$, where the weights $c_i, i = 1, 2, \dots, N$ are obtained by the random-effect meta-analysis model.

Figure 5 shows the estimated pooled causal effects of average all-cause deaths and cause-specific hospitalizations for five heat-related diseases per day per county among 2817 counties across 2000-2016. The curves represent the differences in counts of deaths and hospitalizations per day on average across 2817 counties comparing the counterfactual scenarios where odds of issuing heat alerts were multiplied by factor $\delta \in [\exp(-2.3), \exp(2.3)]$ to the baseline scenario, where the odds of issuing heat alerts remains unchanged ($\delta = 1$). The corresponding point-wise 95% confidence bands of the differences are presented by the dotted lines. The black vertical lines represent the average number of deaths and hospitalizations that could be avoided on a warm season day for a county and their corresponding confidence intervals (CIs) if we had increased the odds of issuing heart alerts by $[\exp(2.3) \approx 10]$ -fold. We find, in general, consistent downward patterns among the pooled causal effect curves for each health outcomes as the $\log(\delta)$ increase above 0 indicating the reductions of all-cause deaths and cause-specific hospitalizations for five heat-related diseases among Medicare enrollees per day per county as $\log(\delta)$ increases. The curves are relatively flat, especially when $\log(\delta) < 0$, and also the confidence intervals contain 0 throughout the range of $\delta \in [\exp(-2.3), \exp(2.3)]$. Quantitatively, we found if we had increased the odds of issuing heart alerts by $[\exp(2.3) \approx 10]$ -fold, on average 0.08 (95% confidence interval (CI): – 0.02 to 0.17) deaths could be avoided for a county

(see vertical black line in Figure 5a). In the calculation of the total events avoidable to heat alerts, we only take into account estimated deaths and hospitalizations avoided among extremely hot days (i.e., the top 5% hottest days with a heat index that exceeded 95% of warm season days in the corresponding county). This gives us approximately 2,329 avoided deaths (95% CI: – 510 to 5,168) among extremely hot days across all 2817 counties in one warm season, and 46,137 avoided deaths (95% CI: – 10,095 to 103,369) for all warm season days. Similarly, if we increase the odds of issuing heart alerts by [$\exp(2.3) \approx 10$]-fold the number of hospitalization avoided are 207 (95% CI: – 122 to 536) for heat stroke; 2,508 (95% CI: – 2,110 to 7,126) for Urinary tract infections; 4,674 (95% CI: – 4,229 to 13,576) for Septicemia; 2,164 (95% CI: – 1,642 to 5,969) for Renal failure; 1,733 (95% CI: – 1,235 to 4,702) for fluid and electrolyte disorders. However, given the wide confidence bands for all these health outcomes, we fail to reject the null hypothesis, i.e., no causal effect of changing the odds of issuing heat alerts on health outcomes comparing $\delta \in [\exp(-2.3), \exp(2.3)]$ vs. $\delta = 1$. The estimated numbers of averted deaths and avoided hospitalizations are with substantial statistical uncertainty. We do find there is large between-county heterogeneity in the random-effect meta-analysis model (P-value of heterogeneity test < 0.001) for all health outcomes. Our findings suggest weak evidence that increasing the odds of issuing heart alerts may bring health benefits to the U.S. Medicare population. However, since heat alerts are rare in almost all counties, we can not extrapolate whether there is a threshold beyond which the increased odds of issuing heat alerts will decrease their effectiveness as people may be less likely to modify their behaviors when the frequency further increases.

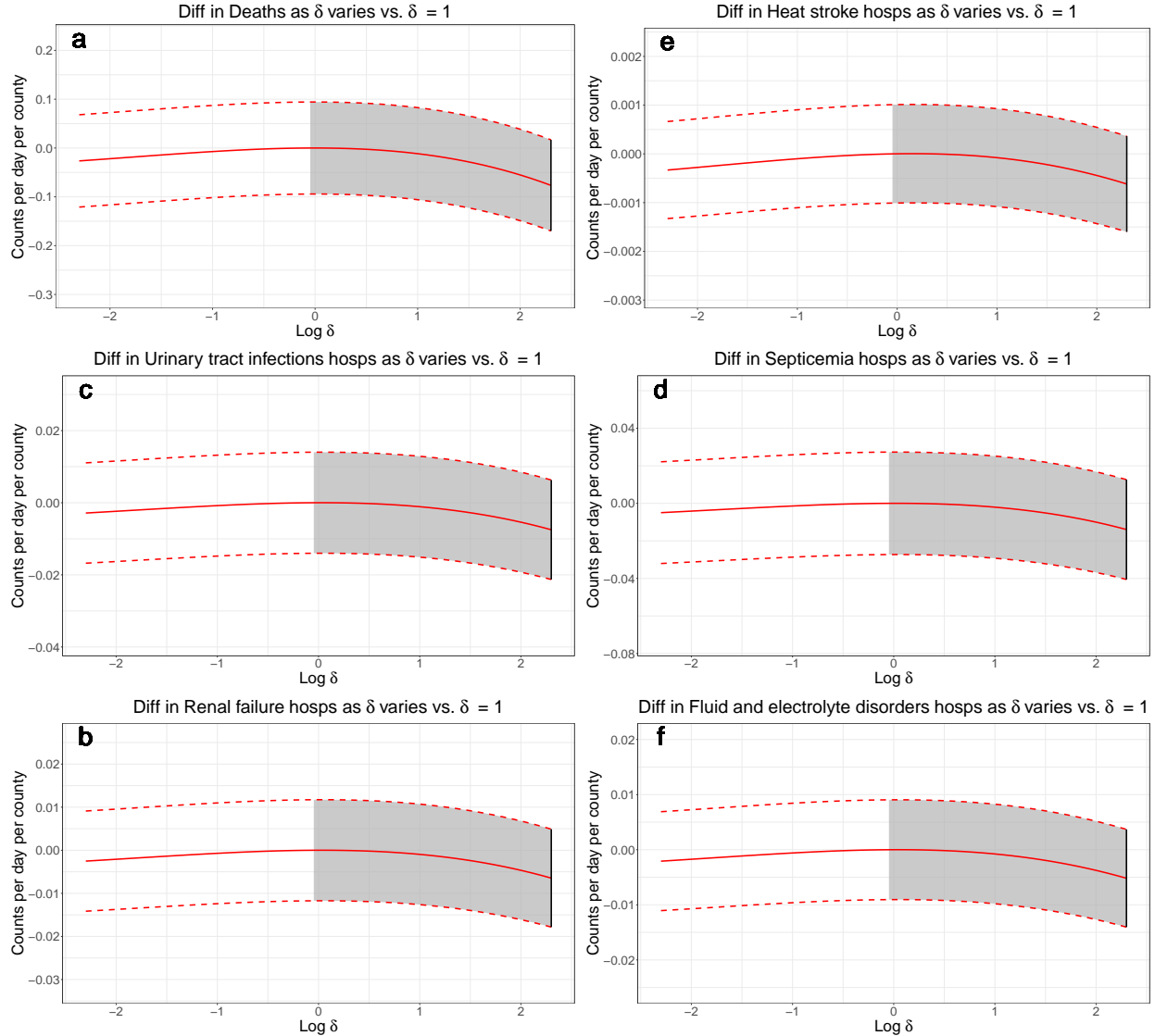


Figure 5: The estimated pooled causal effect curves of average all-cause deaths and cause-specific hospitalizations for five heat-related diseases (heat stroke, urinary tract infections, septicemia, renal failure, fluid and electrolyte disorders) per day per county among 2817 counties. The curves represent the differences in deaths and hospitalizations comparing the counterfactual situations where odds of issuing heat alerts were multiplied by factor $\delta \in [\exp(-2.3), \exp(2.3)]$ to the baseline, where the odds of issuing heat alerts remains unchanged ($\delta = 1$). The corresponding point-wise 95% confidence bands of the differences are presented by the dotted lines. The black vertical lines represent the daily average number of deaths and hospitalizations that could be avoided for a county and their corresponding confidence intervals (CIs) if we had increased the odds of issuing heart alerts by $[\exp(2.3) \approx 10]$ -fold.²⁹

As a sensitivity analysis in the Supplementary Materials, we analyzed the subset of 550 populous counties with $> 100,000$ population sizes. These counties included more than 70% of all-cause deaths and cause-specific hospitalizations observed among the 2817 counties. The motivation for this additional sensitivity analysis was the concern that combining counties with varying population sizes introduces too much heterogeneity in the pooled causal estimates and therefore we examined the subset of populous counties as a sensitivity analysis. As shown in Section S.2, the shapes of the causal effect curves based on the subset of 550 populous counties are very similar to the estimated curves based on data from all 2817 counties. Notably, the width of confidence bands is, in general, narrower than the curves based on data from all 2817 counties, which indicates reduced heterogeneity as expected. Additional sensitivity analysis was conducted where we varied the step size and estimated pooled causal effect curves of 1-step and 6-step estimands. As shown in Supplementary Materials Section S.2, the causal effect of increasing the frequency of issuing heat alerts may have more pronounced effects on health outcomes when considering longer time lags.

8 Discussion

We have developed a causal inference framework for time series data from observational studies. Under this framework, we introduced a new class of time series causal estimands under stochastic interventions. Our proposed nonparametric estimators based on time-varying propensity scores are shown to provide unbiased estimation of the causal estimands with theoretical justification. When observational studies contain time series data from multiple locations (counties in our data application), we link our stochastic intervention framework to the random-effect meta-analysis framework. The ultimate goal in this setting is to obtain a pooled causal estimator that summarizes the potentially heterogeneous causal effects obtained from multiple time series.

The proposed approaches were motivated from our data application where the goal was to assess causal evidence of heat warning effectiveness in reducing morbidity and mortality. We implement the proposed method to estimate the causal effects of NWS-issued heat

alerts on daily average all-cause deaths among Medicare enrollees, and cause-specific hospitalizations for five heat-related diseases (heat stroke, urinary tract infection, septicemia, renal failure, fluid and electrolyte disorders) among Medicare FFS enrollees residing in 2817 counties from 2006 to 2016. The results suggest weak evidence of reductions in morbidity and mortality if NWS increased the odds of issuing heat alerts. However, the results were subject to large statistical uncertainties, probably due to 1) the distinct nature of the demographics for each county 2) the different criteria of issuing heat alerts across the jurisdictions of local NWS offices 3) the low prevalence of the heat alerts in most counties. Importantly, the random-effect meta-analysis model indicated large between-county heterogeneity of the causal effects of NWS-issued heat alerts according to hypothesis test for assumption of heterogeneity in random-effect meta analysis. When we restrict the analysis within 550 counties with $> 100,000$ population size, we find reduced yet still statistically significant heterogeneity of the causal effects of NWS-issued heat alerts across counties. This finding provides important policy implications that the optimal health-based metrics for issuing heat alerts might be specific to geographic locations.

One key distinction of our approach compared to traditional environmental epidemiology methods in the field, is that most time-series studies on heat alerts used matched case-crossover or difference-in-difference designs, where the focus is on the causal effect across case days (i.e., the days with heat alerts), and the number of heat alert days is fixed (Chau et al. 2009, Benmarhnia et al. 2016, Weinberger et al. 2018). In contrast, our analysis focuses on the causal effect of a stochastic intervention, estimating the causal effect as the frequency of the heat alert changes, and as such the counterfactual heat alert days are not fixed. Therefore our results are not directly comparable to previously published studies. While our novel causal inference approach provides new insights about the policy evaluation, there are trade-offs to be considered. First, we expect causal effects defined by stochastic interventions to answer a different policy question than that of a deterministic intervention (Kennedy 2019). The proposed stochastic causal estimand is an intuitive quantity to answer the following causal question “how many adverse health outcomes could have

been averted if we shifted the frequency of heat alerts?” which was the focus of our work. However, other practitioners’ interests may be more aligned with estimating causal effects of deterministic interventions, for instance, “how many adverse health outcomes could have been avoided if the temperature was, on average, one degree lower during extremely hot days (Weinberger et al. 2020)?” In that case, more traditional causal inference methods based on deterministic interventions (Bojinov & Shephard 2019, Bojinov et al. 2020, Rambachan & Shephard 2019) may be used. Second, the random-effect meta-analysis creates a weighted average causal estimand and its corresponding pooled estimator, in which the weights are calculated by the combination of between-study and within-study error variance. For this reason, the weighted average causal quantity is defined on a hypothetical weighted population. Dahabreh et al. (2020) has criticized that standard meta-analyses may produce results that do not belong to a clear target population when each study (counties in our data application) represents a different population and the treatment effect varies across these populations. In the future work, we plan to develop approaches that allow inferences to be transported from multiple time series to a pre-specified target population (Li & Song 2020, Dahabreh et al. 2020). Third, the non-interference assumption may not be met in many environmental health and climate change studies using spatial-temporal data. For instance, the NWS-issued heat alerts in one county may impact people in adjacent counties. In future work, we plan to extend the time series intervention path to a multivariate intervention path defined by random matrices (Papadogeorgou et al. 2020), to potentially overcome the violation of non-interference assumption, and identify direct and spillover effects under this stochastic intervention framework. Fourth, the stable estimation of time-varying propensity score based on observational time series data is challenging since both the time-varying treatment paths and observed confounder set are potentially high-dimensional. We will need to extend the modelling strategy for approximate residual balancing for approximately balancing weights in high dimensions to these observational time series study settings (Athey et al. 2018).

The stochastic intervention framework for time series data introduced in this paper

is the first approach which allows for identifications and estimation of causal quantities defined by stochastic interventions on multiple time series. We believe this statistical framework addresses one of the emerging methodological needs in climate change and environmental health research where researchers often collect time series data from multiple geographic locations seeking causal evidence among representative regions (Liu et al. 2019, Lee et al. 2020). We expect the proposed framework can be adapted without methodological barriers to science and policy-relevant research in political science, economics, and law where considerable amount of spatial-temporal data are generated and collected.

Acknowledgement

The authors are grateful to Jose R. Zubizarreta and Guanbo Wang for helpful discussions. Funding was provided by National Institute of Health (NIH) grants R01 ES029950, R01 AG066793-01R01, R01 ES030616, R01 AG060232-01A1, R01 ES028033, R01 MD012769, R01 ES026217; USEPA grants 83587201-0; and Harvard University Climate Change Solutions Fund. Dr. Wellenius and Dr. Dominici have received consulting income from the Health Effects Institute (Boston, MA). Dr. Wellenius recently served as a visiting scientist at Google, LLC (Mountain View, CA). The authors report that they have no conflicts of interest relevant to this work.

References

- Anderson, G. B., Bell, M. L. & Peng, R. D. (2013), ‘Methods to calculate the heat index as an exposure metric in environmental health research’, *Environmental health perspectives* **121**(10), 1111–1119.
- Athey, S. & Imbens, G. W. (2017), ‘The state of applied econometrics: Causality and policy evaluation’, *Journal of Economic Perspectives* **31**(2), 3–32.
- Athey, S., Imbens, G. W. & Wager, S. (2018), ‘Approximate residual balancing: debiased

inference of average treatment effects in high dimensions', *Journal of the Royal Statistical Society: Series B (Statistical Methodology)* **80**(4), 597–623.

Benmarhnia, T., Bailey, Z., Kaiser, D., Auger, N., King, N. & Kaufman, J. S. (2016), 'A difference-in-differences approach to assess the effect of a heat action plan on heat-related mortality, and differences in effectiveness according to sex, age, and socioeconomic status (montreal, quebec)', *Environmental health perspectives* **124**(11), 1694–1699.

Bobb, J. F., Obermeyer, Z., Wang, Y. & Dominici, F. (2014), 'Cause-specific risk of hospital admission related to extreme heat in older adults', *Jama* **312**(24), 2659–2667.

Bojinov, I., Rambachan, A. & Shephard, N. (2020), 'Panel experiments and dynamic causal effects: A finite population perspective', *arXiv preprint arXiv:2003.09915*.

Bojinov, I. & Shephard, N. (2019), 'Time series experiments and causal estimands: exact randomization tests and trading', *Journal of the American Statistical Association* pp. 1–36.

Borenstein, M., Hedges, L. V., Higgins, J. P. & Rothstein, H. R. (2010), 'A basic introduction to fixed-effect and random-effects models for meta-analysis', *Research synthesis methods* **1**(2), 97–111.

Chau, P., Chan, K. & Woo, J. (2009), 'Hot weather warning might help to reduce elderly mortality in hong kong', *International journal of biometeorology* **53**(5), 461–468.

Dahabreh, I. J., Petito, L. C., Robertson, S. E., Hernán, M. A. & Steingrimsson, J. A. (2020), 'Toward causally interpretable meta-analysis: Transporting inferences from multiple randomized trials to a new target population', *Epidemiology* **31**(3), 334–344.

Daly, C. (2013), 'Descriptions of prism spatial climate datasets for the conterminous united states', *PRISM doc 14*.

- Daly, C., Halbleib, M., Smith, J. I., Gibson, W. P., Doggett, M. K., Taylor, G. H., Curtis, J. & Pasteris, P. P. (2008), ‘Physiographically sensitive mapping of climatological temperature and precipitation across the conterminous united states’, *International Journal of Climatology: a Journal of the Royal Meteorological Society* **28**(15), 2031–2064.
- Granger, C. W. (1980), ‘Testing for causality: a personal viewpoint’, *Journal of Economic Dynamics and control* **2**, 329–352.
- Haneuse, S. & Rotnitzky, A. (2013), ‘Estimation of the effect of interventions that modify the received treatment’, *Statistics in medicine* **32**(30), 5260–5277.
- Hawkins, M. D., Brown, V. & Ferrell, J. (2017), ‘Assessment of noaa national weather service methods to warn for extreme heat events’, *Weather, climate, and society* **9**(1), 5–13.
- Imbens, G. W. & Rubin, D. B. (2015), *Causal inference in statistics, social, and biomedical sciences*, Cambridge University Press.
- Kang, J. D., Schafer, J. L. et al. (2007), ‘Demystifying double robustness: A comparison of alternative strategies for estimating a population mean from incomplete data’, *Statistical science* **22**(4), 523–539.
- Kennedy, E. H. (2019), ‘Nonparametric causal effects based on incremental propensity score interventions’, *Journal of the American Statistical Association* **114**(526), 645–656.
- Kim, K., Kennedy, E. H. & Naimi, A. I. (2019), ‘Incremental intervention effects in studies with many timepoints, repeated outcomes, and dropout’, *arXiv preprint arXiv:1907.04004*.
- Lee, W., Kim, Y., Sera, F., Gasparini, A., Park, R., Choi, H. M., Prifti, K., Bell, M. L., Abrutzky, R., Guo, Y. et al. (2020), ‘Projections of excess mortality related to diurnal temperature range under climate change scenarios: a multi-country modelling study’, *The Lancet Planetary Health* **4**(11), e512–e521.

- Li, X. & Song, Y. (2020), ‘Target population statistical inference with data integration across multiple sources—an approach to mitigate information shortage in rare disease clinical trials’, *Statistics in Biopharmaceutical Research* **12**(3), 322–333.
- Liu, C., Chen, R., Sera, F., Vicedo-Cabrera, A. M., Guo, Y., Tong, S., Coelho, M. S., Saldiva, P. H., Lavigne, E., Matus, P. et al. (2019), ‘Ambient particulate air pollution and daily mortality in 652 cities’, *New England Journal of Medicine* **381**(8), 705–715.
- Naimi, A. I., Rudolph, J. E., Kennedy, E. H., Cartus, A., Kirkpatrick, S. I., Haas, D. M., Simhan, H. & Bodnar, L. M. (2021), ‘Incremental propensity score effects for time-fixed exposures’, *Epidemiology* **32**(2), 202–208.
- Papadogeorgou, G., Imai, K., Lyall, J. & Li, F. (2020), ‘Causal inference with spatio-temporal data: Estimating the effects of airstrikes on insurgent violence in iraq’, *arXiv preprint arXiv:2003.13555*.
- Rambachan, A. & Shephard, N. (2019), ‘Econometric analysis of potential outcomes time series: instruments, shocks, linearity and the causal response function’, *arXiv preprint arXiv:1903.01637*.
- Robins, J. M. & Hernán, M. A. (2009), ‘Estimation of the causal effects of time-varying exposures’, *Longitudinal data analysis* **553**, 599.
- Robins, J. M., Hernan, M. A. & Brumback, B. (2000), ‘Marginal structural models and causal inference in epidemiology’.
- Robins, J. M., Rotnitzky, A. & Zhao, L. P. (1994), ‘Estimation of regression coefficients when some regressors are not always observed’, *Journal of the American statistical Association* **89**(427), 846–866.
- Rosenbaum, P. R. & Rubin, D. B. (1983), ‘The central role of the propensity score in observational studies for causal effects’, *Biometrika* **70**(1), 41–55.

- Rubin, D. B. (1974), ‘Estimating causal effects of treatments in randomized and nonrandomized studies.’, *Journal of educational Psychology* **66**(5), 688.
- Serghiou, S. & Goodman, S. N. (2019), ‘Random-effects meta-analysis: summarizing evidence with caveats’, *Jama* **321**(3), 301–302.
- Spangler, K. R., Weinberger, K. R. & Wellenius, G. A. (2019), ‘Suitability of gridded climate datasets for use in environmental epidemiology’, *Journal of exposure science & environmental epidemiology* **29**(6), 777–789.
- US EPA, E. P. A. (2006), ‘Excessive heat events guidebook’.
- Van der Laan, M. J., Polley, E. C. & Hubbard, A. E. (2007), ‘Super learner’, *Statistical applications in genetics and molecular biology* **6**(1).
- Weinberger, K. R., Harris, D., Spangler, K. R., Zanobetti, A. & Wellenius, G. A. (2020), ‘Estimating the number of excess deaths attributable to heat in 297 united states counties’, *Environmental Epidemiology* **4**(3), e096.
- Weinberger, K. R., Zanobetti, A., Schwartz, J. & Wellenius, G. A. (2018), ‘Effectiveness of national weather service heat alerts in preventing mortality in 20 us cities’, *Environment international* **116**, 30–38.